JOURNAL OF SPATIAL INFORMATION SCIENCE
Number 26 (2023), pp. 53–77
doi:10.5311/JOSIS.2023.26.240

RESEARCH ARTICLE

Surface network and drainage network: towards a common data structure

Eric Guilbert[1], Francis Lessard[2], Naïm Perreault[2], and Sylvain Jutras[2]

[1]Département des sciences géomatiques, Université Laval, Canada

[2]Département des sciences du bois et de la forêt, Université Laval, Canada

Received: July 25, 2022; returned: February 13, 2023; revised: March 11, 2023; accepted: March 20, 2023.

Abstract: The surface network is an application of the Morse-Smale complex to digital terrain models connecting ridges and thalwegs of the terrain in a planar, undirected graph. Although it provides a topological structure embedding critical elements of the terrain, its application to morphological analysis and hydrology remains limited mainly because the drainage network is the most relevant structure for analysis and it cannot be derived from the surface network. The drainage network is a directed, hierarchical graph formed by streams. Ridges of the surface network are not equivalent to drainage divides, which are not contained in the drainage network, and there is no direct association between thalwegs and streams. Therefore, this paper proposes to extend the surface network into a new structure that also embeds the drainage network. This is done by (1) revising the definition of ridges so that they include drainage divides and (2) assigning a flow direction to each thalweg, taking into account spurious depressions to avoid flow interruption. We show that this extended surface network can be used to compute the flow accumulation and different hydrographic features such as drainage basins and the Strahler order. The drainage network extracted from the extended surface network is compared to drainage networks computed with the traditional D8 approach in three case studies. Differences remain minor and are mainly due to the elevation inaccuracy in flat or slightly convex areas. Hence, the extended surface network provides a richer data structure allowing the use of a common topological data structure in both terrain analysis and hydrology.

Keywords: Morse-Smale complex, surface network, drainage network, digital terrain model

1 Introduction

Topography relies mainly on the digital terrain model (DTM) to study landforms and land features. But the need to describe landform characteristics and their relationships in formal structures arose much earlier. In their review, Clarke and Romero [9] traced back to original works from Cayley [8], who first described a surface from its critical points (pits, peaks and saddles) and lines (ridges and thalwegs), and Maxwell [24] who also established that critical lines segment the terrain into dales and hills. These critical elements provide a topological structure describing terrain saliences that can be associated to landforms. Morse [25] later proposed a theory that analyses the topology of sufficiently smooth manifolds, the Morse functions, and allows for the definition of the *Morse-Smale complex* (MSC) connecting all critical elements. In the case of the terrain, Pfaltz [28] introduced the concept of *surface network*, a tripartite graph that connects critical lines and points. The terrain is seen as a Morse function and the surface network is a MSC computed from the terrain.

While the DTM is commonly used in spatial information science and more generally in environment science for terrain analysis, the MSC was mainly used for terrain and other surface visualization and simplification in other fields of application. Rana [30] presented two main reasons for this. A first reason relates to the difficulty to build a topologically correct network. In many domains, the surface can be defined by a mathematical function or by smooth, regular shapes with sharp edges, as in computer-aided design or computer graphics. However, features on a natural terrain are not always clearly marked and this uncertainty creates topological inconsistencies. The issue is due to the inherent difficulty in estimating the gradient on discrete surfaces that include noise. This is particularly true for high-resolution DTMs obtained from lidar data that have a rough appearance [22].

A second reason is that, in geomorphology, most common features that are sought for to analyse a terrain are hydrological features. Geomorphologists and hydrologists mainly rely on the computation of the drainage network to explain the features on a surface, especially in fluvially eroded terrains. The drainage network is composed of streams that form a directed, hierarchical graph. Tributary streams connect at main streams at confluence points and their hierarchical position can be defined by an order such as the Strahler order [33].

The surface network and the drainage network share similarities. Thalwegs and streams are both defined as lines of converging flow while ridges are lines of diverging flow, as are drainage divide. The drainage network is commonly used as a way to extract thalwegs while ridges are extracted by computing the drainage network on an inverted DTM [9]. However, in the drainage network, the relevance is not put on the same features and both networks are computed with different approaches.

The drainage network is extracted by computing the flow direction and the flow accumulation [27]. The approach simulates a flow on a DTM and computes the amount of water accumulated in each pixel. In the common D8 approach [27], the flow is directed from one pixel to the next among the eight possible neighbors according to the steepest slope. Because the flow direction is constrained by the grid cells and very sensitive to noise, other approaches were proposed. [13] proposed a stochastic method to correct the bias between the grid orientation and the slope aspect. Some authors computed flow directions along the gradient and shared the flow between different pixels [29,35]. More recently, [23] presented a different approach, specific to lidar-derived grid DTM where a flow direction and a flow path are interpolated from the lidar points. They thus form chain vectors whose direction is not constrained by the grid. However, in practice, the D8 method remains the most com-

monly used because allowing multiple flows and thus dispersion of the flow from one pixel is not consistent with the physical definition of catchment areas [35]. Approaches with a single flow direction are also preferred for processing high-resolution DTM because they are simpler and faster [2].

Flow accumulation is given by the amount of water that flows through each pixel. Accumulation values higher than a threshold are considered as streams and a drainage network is vectorized from these pixels. Flow accumulation methods require the removal of small depressions that interrupt the flow. This is done by drainage enforcement techniques that remove local minimums. The most common technique consists in filling these spurious depressions by raising the elevation of the points within [19]. Hence, most pits that mark these depressions on the surface network are seen as spurious pits that hinder the computation of the flow direction. Furthermore, while saddles are seen as critical elements of the surface, they are not seen as significant features of the terrain [6] and are not considered at all in the drainage network.

The flow direction is also used to compute drainage basins, formed by pixels whose flow contributes to the same outlet. Limits of drainage basins correspond to drainage divides. While these divides can be seen as ridges, their computation depends on the accumulation threshold. However, whether ridges are computed from the inverted DTM or as the drainage divides, ridges and streams are disconnected and do not form a connected graph, even less a simplicial complex. Hence, while the drainage network is commonly used in terrain analysis, it does not provide a topological structure as rich as the surface network.

On the other side, the MSC does not provide a drainage network because it is an undirected graph. Because of spurious pits, the flow direction cannot be inferred directly by directing the thalwegs according to the slope. Since there is no hierarchy in the network, no flow accumulation can be defined either.

Nonetheless, the surface network is still a relevant structure that contains salient features of the terrain. It has been used for example to preserve features in terrain simplification [12], and to extract topographical eminences [32] and submarine canyons [11]. Thus, we propose in this paper to extend the definition of the surface network to allow for the extraction of the drainage system from the surface network. We consider that such a network would yield several benefits: (1) it would provide a common structure that can be used in topography and in hydrography, (2) drainage computation does not require drainage enforcement altering the DTM and includes both ridges and streams in the same structure. Therefore, it will guarantee the topological consistency of all terrain elements and provide explicit relationships between streams, ridges and basins. Such a structure can easily be stored in a database for query and extracting different terrain representations.

The new surface network definition still relies on the existing surface network but (1) revises the definition of ridges and dales so that they fit with drainage divides and allow for the computation of drainage basins; (2) directs the thalwegs according to the flow direction and by taking into account local depressions identified by pits; (3) computes the flow accumulation from dales. This structure guarantees the topological consistency between all elements of the drainage and can be used to retrieve the drainage network or drainage basins at any level of detail (according to the Strahler order or the flow accumulation).

The paper is organized as follows. The next section describes the surface network theory on which this work relies. Section 3 presents the new definition of the surface network, with directed thalwegs and a more generic ridge definition. Section 4 converts this network

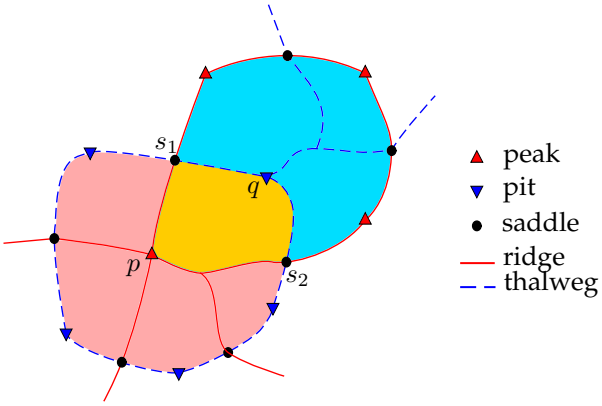

Figure 1: Surface network. The Morse-Smale cell (yellow) is obtained by the intersection of the blue dale containing pit q and the red hill containing peak p

into a drainage network from which different elements such as drainage basins or Strahler orders of streams can be derived. Results are compared with drainage networks computed by flow accumulation. The final section gives concluding remarks and perspectives for future works.

2 The surface network

2.1 Definition

A surface network is a tripartite graph where vertices are peaks, pits and saddles of the terrain and edges are its ridges and thalwegs (Figure 1). Surface networks are grounded in the Morse theory [10] and are a special case of a Morse-Smale complex applied to a DTM. The terrain is considered as a 2D manifold defined by a scalar function $z = f(x, y)$ over a domain $D \subset \mathbb{R}^2$. If f is twice differentiable, critical points are points where the gradient is zero and a critical point is called degenerated if its hessian is equal to zero. The function f is a Morse function if none of its critical points is degenerated. A critical point p of a 2D Morse function f can be of three kinds:

- a pit: the point p is a local minimum;
- a peak: p is a local maximum;
- a saddle: f is convex in one direction and concave in another direction at p.

Ridges on the terrain are lines of diverging flows while thalwegs are lines of converging flows. This means that a flow line can never cross a ridge or a thalweg. Consequently, when a flow reaches a thalweg, it will keep flowing until reaching a pit. This means that a thalweg always connects to a pit at its lower end. Similarly, by following a gradient path, ridges always connect to a peak at their upper end. Based on the definitions above, a surface network always satisfies the following properties:

- Ridges and thalwegs intersect at saddle points only;
- A ridge connects a peak and a saddle;

- A thalweg connects a pit and a saddle;
- At a saddle, the number of ridges is equal to the number of thalwegs;
- When turning around a saddle, critical lines alternate between ridges and thalwegs.

Finally, the surface network satisfies the Euler-Poincaré characteristic for closed 2D manifolds so that:

$$\#\text{peak} + \#\text{pit} - \#\text{saddle} = 2 \tag{1}$$

Since a terrain is usually not a closed surface, a virtual pit located below the terrain is added to satisfy the characteristic.

The surface network provides a full decomposition of the terrain into cells corresponding to dales (ascending cells) and hills (descending cells). Each pit of the terrain is surrounded by ridges that form a dale, an area where all flows converge to the pit. Respectively, each peak is surrounded by thalwegs that delineate a hill. The intersection of a hill and a dale forms a Morse-Smale cell, a cell that contains all the flows starting from a peak and reaching a pit, corresponding to a hillslope as the yellow cell of Figure 1 contains all the flows running from p to q.

2.2 Construction of the Morse-Smale complex from a raster DTM

Surface networks and more generally Morse-Smale complexes are defined for smooth surfaces. When working on terrains modeled by a grid or a raster, the height function is discretized, bringing numerical issues in the computation of the network. Different strategies exist to compute the Morse-Smale complex [10]. Methods specifically developed for raster DTMs start by extracting saddle points and trace critical lines starting from the saddles up to the peaks or down to the pits. Since critical lines are initiated at saddle points, the efficiency of the method relies on a proper detection of saddles. Furthermore, while their definition is clear, their computation on a discrete surface relies on a gradient approximated by finite differences. This leads to singular cases such as overlapping or crossing lines that do not occur in theory.

In the case of a grid or raster DTM, the terrain is considered either as a piecewise bilinear surface [26, 31] or a piecewise linear surface [34]. In the first case, each cell formed by four pixels is considered a bilinear function. Saddles can be located at pixels or inside the cells but not on their edges. Ridges and thalwegs can cross cells along the steepest slope. While the method presented in [26] is robust enough to prevent ridge and thalweg intersections, bilinear approaches present several limitations for their application to high resolution DTMs. First, critical points and lines are computed at sub-pixel accuracy. While this may be more precise, on high-resolution DTMs, it may lead to spurious details such as several thalwegs running in parallel a few centimetres apart along a valley floor. Second, critical lines are computed by a gradient descent and thus their calculation depends on a descent step. While it yields smooth lines, conflicts between two thalwegs or two ridges may occur and it is difficult to address the junction of two lines [16].

In linear models, the DTM is triangulated by inserting a diagonal in each cell to provide a piecewise linear surface. The number of neighbors of each pixel varies between four and eight and depends on the triangulation. [34] do not propose any specific triangulation approach. Following the same approach, [17] propose to connect each pixel to the lowest pixel of a cell and thus facilitate the computation of converging flows. While this approach limits the number of pits and thus the number of spurious pits, it does not maximize the number

of saddles. Because critical lines are initiated at saddles, this method does not detect all possible critical lines. Thalwegs and ridges are computed in a second step. Starting from a saddle, ridges are lines following the path of steepest ascent while thalwegs follow the path of steepest descent. In [34] and subsequent approaches, lines connect pixels along triangle edges but cannot cross the triangles. This means that they do not follow the gradient path. Other approaches such as [7] follow the line of steepest descent or ascent by inserting new nodes and splitting the triangles. However, such an approach was developed firstly for triangulated irregular networks. Such lines would no longer match the grid structure of the raster, loosing the benefit of a regular structure. Furthermore, in high-resolution DTMs, this may lead to unnecessary details and to numerical inconsistencies with very small triangles.

In a surface network, two ridges or two thalwegs can overlap and join the same peak or pit. Topological consistency is preserved either by considering that the two lines run side by side to the same node or by introducing a junction node and initiating a new line after the junction [7]. However, intersections outside a saddle can also occur between a ridge and a thalweg. These cases are due to the discrete representation of the gradient. [31] proposed to insert pseudo-saddles at these points to preserve the consistency of the network, although these intersections are artefacts that do not reflect some real terrain characteristics.

Recently, a new approach specific to raster DTM was proposed in [16]. Their method aims at ensuring the topological consistency of the network. The method triangulates the DTM in order to preserve as many saddles as possible and maximize the number of critical lines. Since critical lines follow the triangulation edges, which is not the gradient path, a correction is applied to take into account the offset that is added at each step. The method computes thalwegs first and makes sure that no intersection with thalwegs occurs when computing ridges. As in [7], the method introduces nodes when critical lines merge. They are confluences where two thalwegs merge and junctions where two ridges merge. Among the previous methods, it is also the only one to compute dales and hills.

Nonetheless, the surface network is not equivalent to the drainage network as mentioned earlier. First, while streams can be supposed to run towards and through valley thalwegs, ridges are not equivalent to drainage divides [6]. Hence the definition of ridges should be extended to drainage divides that separate the flow and delineate basins. Second, thalwegs form an undirected network and should be directed according to the flow. Because of spurious pits that interrupt the streams, the flow may go against the slope to provide a way out of these pits.

3 The extended surface network

3.1 Differences between the MSC and the drainage network

A drainage network can be considered as a directed graph with up to four types of nodes:

- A spring is a node that initiates a flow but does not receive any flow;
- A sink is a node that only receives flow;
- A confluence where several streams arrive and one depart;
- A diffluence is a node where a stream arrives and several streams depart.

Segments between two nodes are streams directed according to the water flow. Except in special cases of endorheic basins, sinks are on the boundary of the domain. As mentioned in the introduction, the flow directed from one pixel can be unique, as in the D8 approach

[27] or can be multiple as in [29]. In the first case, only one direction is possible. There are confluences but no diffluence is found. In the second case, a stream can have distributaries and thus, there are diffluences.

In a MSC, most saddles are connected to exactly two thalwegs and would correspond mainly to transfluences. Thus, they are not relevant in a drainage network. Only multiple saddles can correspond to confluences in the drainage network. On the opposite, confluences in the drainage network are not critical points of the MSC. They are only considered in some computation approaches to avoid overlapping thalwegs in the data structure. As mentioned before, most depressions of the DTM are considered spurious in the drainage network. They are filled or breached in order to compute a proper flow direction [21]. Hence, pits on the surface network mostly mark spurious depressions and are not sinks. Thus, they correspond to transfluences or confluences depending on the number of thalwegs they connect. Unless another pit is identified as a sink, the only sink in the surface network should be the virtual pit to which all streams flow.

Furthermore, the drainage network does not provide any computation method for flow accumulation. The flow accumulation is the amount of water that runs through a cell of the network. It is given by the area of the drainage basin at this point. Limits of the drainage basin are the drainage divides. These divides should be initiated at the confluence of two thalwegs to separate their respective drainage basins. However, ridges delineate the flow between ascending cells. As shown in Figure 1, the blue cell contains all the flow lines that converge to q. They do not separate the flows converging to each thalweg. In order to embed both MSC and drainage network in the same structure, a broader ridge definition is required, leading also to a new dale definition.

In the remaining of this section 3, we extend the definition of the surface network so that it embeds the surface network (i.e. the MS complex as defined in [28]) and the drainage network. The resulting extended surface network (ESN) is still a simplicial complex composed of a ridge network and a thalweg network. In order to extract the drainage network, we also provide a new definition of the flow accumulation and define the thalweg network as a directed graph. We present the new definitions of ridges and dales and how they are computed from a raster DTM in Section 3.2. Sections 3.3 and 3.4 present how the flow is directed and the accumulation is computed.

3.2 Ridges and dales

3.2.1 Definitions

As mentioned before, the new surface network extends the MSC. Hence, all elements of the MSC are found in the ESN and pits, peaks and saddles are still critical points of the ESN.

The ridge definition is extended to include divides as a type of ridge. Considering a critical point connecting at least two thalwegs, divides should be traced to separate the areas that contribute to each thalweg. This means that a divide should be traced starting from the node between each pair of thalwegs. Ridges already divide the flows at saddles. However, divides should also be added at other points where several thalwegs join. Thalwegs could be either starting or ending at these points.

More generally, ridges are initiated at all nodes connected to a thalweg. As such, ridges are initiated at points where several thalwegs intersect, corresponding to confluences. Confluences were already identified in [16] to avoid storing overlapping thalwegs. In the ESN, such nodes are now considered as critical points of the network to which thalwegs start

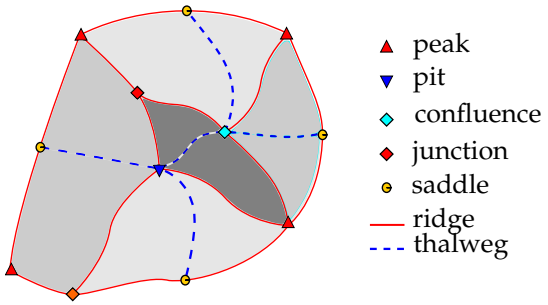

Figure 2: Ridges and dales of a drainage network. Ridges are initiated at saddles, pits and confluences, delineating a dale around each thalweg. Dales are shown in different shades.

or stop. Therefore, a thalweg can start at a saddle or at a confluence and end at a saddle, a confluence or a pit. For example, in Figure 2, three thalwegs join at a confluence: two coming from saddles, and one going to the pit. Thus, three ridges are initiated at this node. Similarly, three ridges are initiated at the pit.

In the MSC, the number of ridges starting at a saddle is equal to the number of thalwegs starting at the saddle. In the ESN, a ridge can start at a saddle, a confluence or a pit and can end at a saddle, a confluence or a peak and the number of ridges starting at a node is equal to the total number of thalwegs starting or arriving at this node.

Because of the less restrictive connection rules between critical points and lines, the ESN is not a tripartite graph. This new definition of ridges also leads to a greater number of ridges because a thalweg initiates two ridges: one at its starting node and one at its end node. Therefore, the ESN contains twice as many ridges as thalwegs:

$$\#\text{ridge} = 2\#\text{thalweg} \tag{2}$$

In a MSC, an ascending cell is a surface defined by all the flow lines coming from a pit. They are delineated by ridges and form a partition of the terrain. In the ESN, dales are still delineated by ridges. However, they are no longer centred on pits but on thalwegs and are defined for each thalweg by all the flow lines that run into the thalweg. Hence, each thalweg is associated to a dale in a one-to-one relationship (Figure 2) and the dale is connected to both ends of the thalweg.

This last point means that a thalweg partitions a dale in two slopes. These slopes are also obtained by the intersection between a hill and a dale. Like the MSC, the ESN is a simplicial complex and can be decomposed into a hill complex and a dale complex. The hill complex provides the same decomposition as the descending manifold. The dale complex provides a decomposition in smaller cells than the ascending manifold. The ESN can be converted into a MSC by regrouping dales into ascending cells: for a given pit, one retrieves all the thalwegs whose flow converges to this pit and merges the dales of all these thalwegs.

As in the MSC, the ESN can contain dangling thalwegs and ridges. A dangling line is a line that is not located on the boundary of a hill or dale. A dangling thalweg (resp. ridge) connects a hill (resp. dale) to a critical point or to a hill (resp. dale) that represents a hole. For example, Figure 3 shows a dangling thalweg connecting a saddle and a pit. The dale associated to the thalweg is in grey. Figure 4 shows an example of a dangling thalweg (thalweg 1) ending at a confluence. The hill formed by thalwegs 2 and 3 is a hole

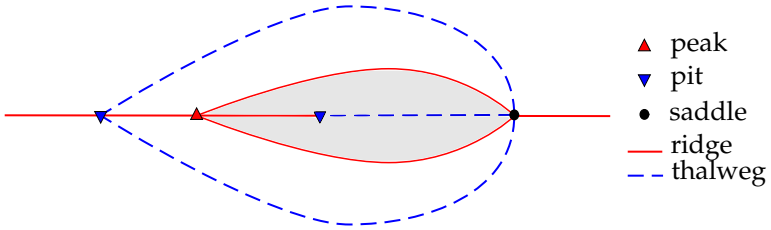

Figure 3: Dangling ridge and thalweg. The grey area is a dale.

included in a larger hill. In the case of Figure 3, the dale of the dangling thalweg is also the ascending cell of the pit. This ascending cell is properly defined by the two ridges starting at the saddle. In the ESN, adding the dangling ridge is required to respect the constraints above: it enforces equation (2), it connects both ends of the thalweg to the dale and the thalweg separates the dale in two slopes.

3.2.2 Construction on a raster DTM

To compute the ESN on a raster DTM, we follow a similar approach as [16] where the raster is seen as a regular grid. The method relies on the triangulation of the grid and the existence of a virtual pit that closes the surface. Critical lines follow triangulation edges and may overlap under some conditions. The method also computes hills and dales.

The first steps for the construction of the ESN are the same as for the MSC:

1. Saddle and pit detection
2. Thalweg computation and confluence detection
3. Hill computation
4. Peak detection

Saddles can be computed in different ways, as in [16], where their number is maximized, or as in [17] to limit the number of spurious pits. Confluences are detected during the thalweg computation: each time a thalweg reaches another thalweg, a new confluence is created. This imposes that thalwegs are computed before ridges. Computation of a steepest path for thalwegs can be done by choosing the pixel with the steepest slope [17] or by staying close to the gradient [16]. The second method is mainly relevant when the slope is smooth and regular. If the terrain is rough, correcting the error between the steepest slope and the gradient is not relevant and the first method is more appropriate. A stochastic approach such as [13] could also be used but it would mean that the same algorithm does not yied the same result each time.

Ridge computation in the ESN differs from the MSC in their initialisation and in their end. Ridges are initiated along the steepest slope upward between two thalwegs at saddles but also at pits and confluences. Consistency between ridges and thalwegs is maintained by imposing a ridge remain in its hill. Around a node, each ridge belongs to a different hill. An exception is if one thalweg is a dangling thalweg. In that case, both ridges on each side of the thalweg belong to the same hill and ridges have to be marked as standing on the left or right of the thalweg. Ridges normally run up to a peak but, in order to avoid overlapping ridges, junction nodes are inserted. In [16], a junction could have the same

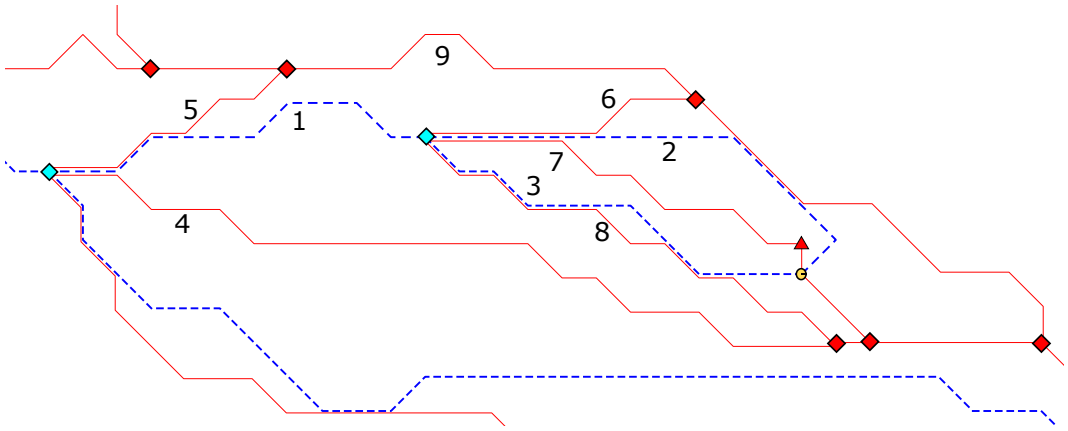

Figure 4: Thalwegs 1, 2, 3 partially overlapped by ridges 4, 5, 6, 7, 8. Thalweg 1 is a dangling thalweg.

position than a confluence. In the ESN, this does not happen anymore because ridges are directly connected to the confluence.

As with other methods where critical lines run along edges of the triangulation, ridges and thalwegs can overlap. This does not hinder the topological consistency because each ridge is located either on the left or right of a thalweg. Figure 4 shows an example of a dangling thalweg. Ridges 4, 5, 6 and 8 are all located in the same hill. Ridges 5 and 6 are on the right of thalweg 1 and ridges 4 and 8 are on its left. Ridges 6 and 7 both overlap thalweg 2 and are in two different hills.

Dales are computed by starting from the node at the start of a thalweg and walking along ridges until coming back to this node. In Figure 4, the dale of thalweg 1 is formed by the sequence of ridges 5-9-6-8-4. Because ridges and thalwegs can overlap, a dale can have an area equal to 0. Both ends of the thalweg are always located on the boundary of the dale so that the thalweg splits the dale into two cells. These cells are the left and right slopes of the thalweg and contain the flow running from either side of the thalweg.

At this stage, the ESN is a simplicial complex but thalwegs still form an undirected, unweighted graph. The following sections present how to direct the flow in the thalwegs and to compute the accumulation. Both operations are done on the ESN directly and do not require the DTM.

3.3 Puddle computation

In the ESN, each thalweg corresponds to a potential stream segment and must be directed according to the flow. The flow can simply be defined by directing each thalweg from its higher end to its lower end. But, as with flow accumulation methods, the flow would be interrupted by spurious pits along the thalwegs. These pits more than often correspond to some local minima found in nearly flat parts of the terrain. A correction to the flow direction needs to be brought in these cases to guarantee that the flow run uninterrupted from a spring to an outlet.

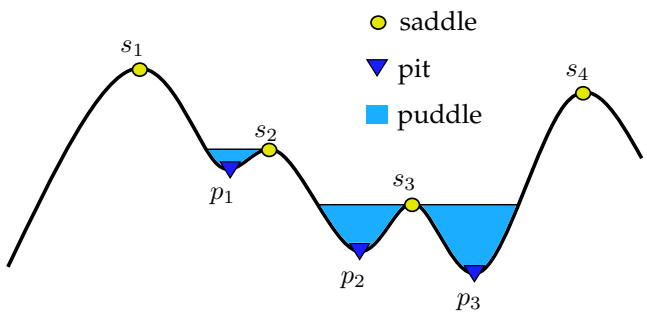

Figure 5: Puddles defined by pairs of saddle and pit along a thalweg. Saddle s_3 belongs to two puddles.

In order to compute a flow out of such spurious pits, we introduce the concept of *puddle*. Puddles are found at pits that prevent the flow to go further down. They correspond to the idea that the water level rises in a pit, forming a puddle until reaching an outlet. In this way, it matches the definition of closed depression given by [36] that are filled and removed from the DTM. However, the puddle is defined solely by a set of nodes and the thalwegs they connect. A puddle includes at least two nodes, a pit and one outlet from which the flow comes out. The puddle definition also includes one node outside the puddle in which the water pours in after the outlet, that we call the *pouring node*. A puddle can have only one outlet and pours into only one pouring node. For example, in Figure 5, a first puddle is defined by pit p_1 and saddle s_2. Its pouring node is pit p_2. The node p_2 is also the pouring node of the puddle formed by p_3 and s_3. Obviously, outlets are saddle points since they correspond to points of maximum height located along the thalwegs.

Puddles are initialised for each pit in the domain (excluding the virtual pit and any other node that is identified as a sink) and are extended by adding adjacent nodes recursively until a node n of the puddle has a lower neighbor located outside the puddle. This node n is the puddle outlet. The pouring node is defined by the next node where the flow runs from the outlet. If there are several possible pouring nodes, which occurs when the saddle is connected to three or more thalwegs, the flow follows the steepest slope. The generic algorithm for computing a puddle starting from one or several nodes is given by algorithm 1. The algorithm proceeds by taking the neighbors of the starting nodes. A neighbor that is higher than a node is in the same depression and it belongs to the puddle if it is lower than the outlet. A neighbor that is lower and outside the puddle is not in the same depression and can be the pouring node.

As shown in Figure 5 with s_3, two puddles can have the same outlet or, more generally, pour into each other if each pouring node is located in the other puddle. In that case, the flow would be interrupted or would loop between the two puddles. These puddles need to be merged into a larger puddle with its own outlet. Merging two puddles is done with the same algorithm 1 but by taking the nodes from both puddles in input. Three cases are considered.

- Two puddles share the same outlet. The new puddle containing all the nodes from both puddles is computed, looking for a new outlet;
- Puddles have different outlets but share the same pouring node (Figure 6). If there is no other thalweg in which the flow can pour, the flow is interrupted at the pouring

Algorithm 1 Computation of a puddle from a set of nodes

```
function COMPUTEPUDDLE(list of nodes puddle)
    S ← puddle                                   ▷ S is a stack used to visit all nodes in the puddle
    outlet ← highest point                       ▷ initialised to the highest point on terrain
    pouring ← highest point                      ▷ the pouring node
    while S do
        n ← S.pop()
        lowernode ← n.getLowerNeighboursOutsidePuddle(puddle)
                  ▷ lowernode is the list of nodes lower than n that are not in the puddle
        highernode ← n.getHigherNeighboursOutsidePuddle(puddle)
                  ▷ highernode is the list of nodes higher than n that are not in the puddle
        for ln in lowernode do
            if n.z < outlet.z or (n.z =outlet.z and slope(n → ln) > slope(n → pouring)) then
                  ▷ n is lower than the current outlet and its neighbour ln is even lower
                outlet ← n                       ▷ n is the new outlet
                pouring ← ln                     ▷ ln is the new pouring node
            end if
        end for
        for hn in highernode do      ▷ hn is higher than n but still in the same depression
            puddle.append(hn)                    ▷ hn is added to the puddle
            S.append(hn)
        end for
    end while
    for n in puddle do
        if n.z > outlet.z then                   ▷ remove all the nodes above the outlet
            puddle.remove(n)
        end if
    end for
    return puddle
end function
```

node. A new puddle is computed with the nodes of both puddles and the pouring node;

- For two puddles A and B, the pouring node of puddle A is a node of puddle B and the pouring node of puddle B is a node of puddle A. Such a case would create a loop in the stream network. The new puddle is computed by taking all the nodes from both puddles.

Since creating new, larger puddles can lead to new conflicts with other puddles, the process is repeated until no further merge can be done. For example, in Figure 5, the two puddles (p_2, s_3) and (p_3, s_3) are merged into one puddle (p_3, p_2, s_3, s_2) which is in turn merged with the puddle (p_1, s_2) into a larger puddle whose outlet is s_4. At the end of this step, all puddles of the surface network have been identified and form disjoint subsets in the network.

As mentioned earlier, puddles are mainly observed in flat areas. Figure 7 shows a valley floor corresponding to a wetland. The number of thalwegs and puddles in the floor is far

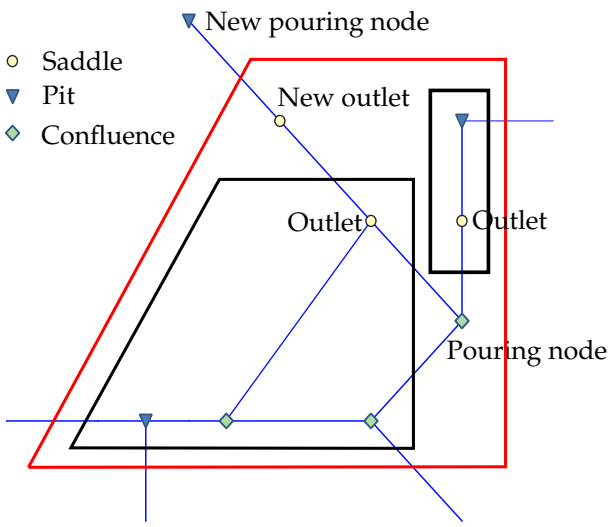

Figure 6: Two puddles (black polygons) sharing the same pouring node. Outlets are the saddles in each puddle. The new puddle is the red polygon.

higher than on the slopes. The figure also shows that many puddles are found along the road embankment on the left.

3.4 Flow direction and accumulation

Computing the flow direction consists in directing each thalweg. For all streams that are not located in a puddle, the thalweg is oriented towards the lowest end. In puddles, thalwegs must be directed towards the outlet. Computation inside a puddle is done by starting from the outlet and recursively directing all the thalwegs towards the outlet.

A check for the existence of loops is performed in the directed network. While all flows should converge outside the puddles towards a sink, such loops occur in flat terrains where the flow out of a puddle is sent back to another node inside the puddle that is exactly at the same height. Such loops are corrected by adding the pouring node to the puddle in order to extend it and include both nodes at the same height.

Once the direction is set, springs can be identified as nodes to where no flow converges. More specifically, springs are saddles that do not receive any flow and pits that connect to only one thalweg. These pits are inside a puddle where the stream has been directed from the pit towards the saddle.

In a drainage network, the flow accumulation of a point along a stream is the amount of water that flows through this point from above. In a raster DTM, flow accumulation is given by the number of pixels whose flow runs through this point. In the ESN, flow accumulation is computed not per pixel but per thalweg and corresponds to the accumulation at the outlet of the thalweg.

The thalweg is a line to which all flows within a dale converge. Hence, the flow accumulation of a thalweg is given by the flow coming from thalwegs upstream and the flow within its dale. The flow in a dale is given by the dale area while the flow coming from

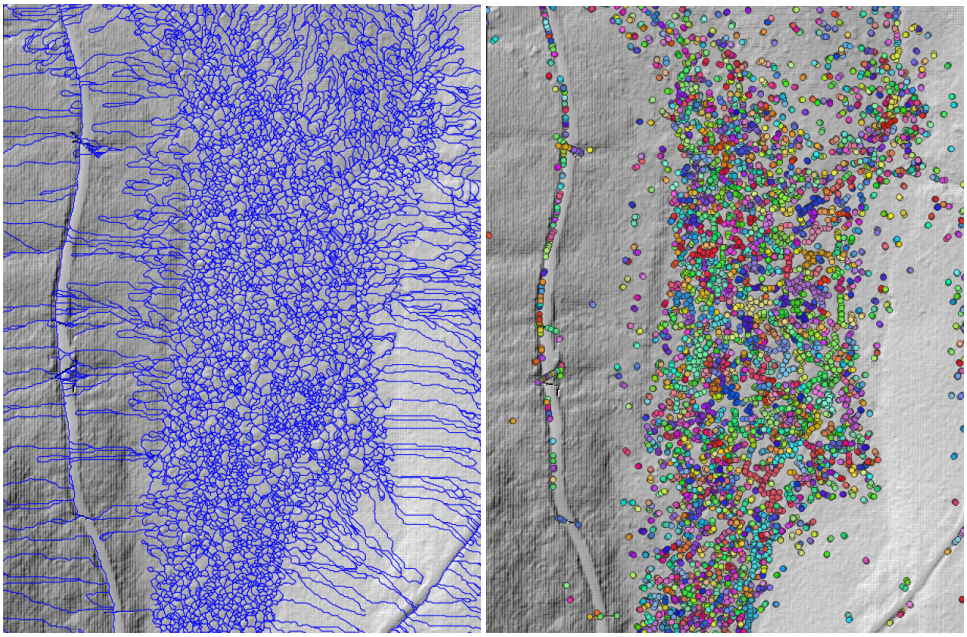

Figure 7: Left: thalwegs computed in a valley. Right: nodes from puddles (in color).

upstream is the accumulation measured at thalwegs directly above. Thus, flow accumulation is computed recursively as the sum of the areas of all dales located upstream and is recorded as a thalweg attribute.

While no cycle occurs in the network, the flow at a node may separate in multiple directions. This case occurs for example when a saddle is the end point of a thalweg and the starting point of two other thalwegs. Hence, two options are possible: if the user allows distributaries, the flow is distributed between them in proportion to the slope: steeper thalwegs receive more flow than the others [29]. This means that a thalweg can have a lower accumulation than its upper thalweg. If, as is often the case in practice, distributaries are not allowed, the thalweg with the steepest slope receives all the flow.

4 Application to drainage computation

4.1 Drainage features

4.1.1 Drainage network

The drainage network is extracted from the ESN. Because the ESN already provides the flow direction and the flow accumulation of each thalweg, the drainage network is computed by defining an accumulation threshold and selecting all the thalwegs with a higher accumulation. This threshold is set by the user, depending on the type of flow regime considered in the analysis and on the characteristics of the terrain.

4.1.2 Strahler order

The Strahler order defines a hierarchy between the streams. Streams connected to a spring are of order 1. Each time two streams of the same order merge, the order of their descending stream is increased. Hence, the closer to the network outlet, the higher the order. Because the Strahler order is defined for streams only, it depends on the accumulation threshold defined previously by the user.

The Strahler order is computed by starting from the springs of the network. Only thalwegs whose accumulation is high enough to form a stream have a Strahler order. Hence, the order is set to 0 at thalwegs starting at a spring and turns to 1 only when the accumulation becomes large enough.

Allowing distributary streams in the network also affects the Strahler order. If two distributaries merge again, increasing the order of the new stream would lead to an inappropriate increase of the Strahler order. Hence, computation of the Strahler order is done by checking if two streams share a common spring. In that case, the order is not increased.

4.1.3 Drainage basin

The drainage basin of a point along a stream is the area of all flows that converge to that point. In our surface network, the thalweg being the basic stream unit, a drainage basin is the area of all flows converging to a thalweg and is computed in a similar approach as the flow accumulation: it is the union of all the dales located above a thalweg.

Basin calculation makes use of the dale partition of the terrain to avoid geometrical calculations. Each dale is defined by a series of directed ridges. A ridge that separates two dales appears in one dale in one direction and in the other dale in the other direction.

The algorithm first retrieves all the dales located upstream of the thalweg to obtain a list of directed ridges. Dangling ridges are removed from this list because they do not separate two dales. All ridges that appear twice in the list in two different directions are inner ridges. Ridges that appear only once are the ridges on the boundary of the basin. Hence, only these ridges are kept and ordered to form the basin polygon.

If distributary streams are not permitted, drainage basins of two thalwegs cannot overlap, unless one thalweg is located in the basin of the other. Two adjacent basins share a common boundary defined by a common set of ridges. If distributaries are allowed, two adjacent basins can overlap and the overlapping area corresponds to the area that contributes to both basins.

4.2 Case studies

The method was implemented in Python using the OGR/GDAL libraries to handle data files. It extends the code presented in [16] that computes a MSC from a raster DTM by adding the new elements presented in section 3. The code is available at https://github.com/ericguilbert/SurfaceNetwork.

Case studies are presented to validate that the ESN can be used to extract different elements of the drainage system. We first extract the drainage network and compare it with a drainage computed by flow accumulation. We also compute the Strahler order of the streams and compute several drainage basins.

Three datasets were used to assess the results. They are DTM at one-metre resolution from three different areas in Québec province, Canada. Data are provided by the Ministère

des Forêts, de la Faune et des Parcs du Québec and are freely available online[1]. The DTM were built from airborne lidar point clouds. The raw point clouds are at a resolution of at least 4 points per square metre. Ground points were filtered from the point clouds and the DTM were interpolated by binning. The terrains are located in forest areas and contain some forest tracks with culverts which are not visible on the DTM but can reroute the flow [3]. Their positions were obtained from observations on the field and the terrain was burnt at these places.

The three terrains correspond to three drainage basins and have different characteristics. The ruisseau des eaux volées basin (Berev) is located in the Laurentian Mountains, with elevations between 600 m and 900 m and a till varying from thin to thick based on elevation and slope [5]. The DTM covers about 10 km^2. The second DTM covers the drainage basin of the Kinonge river in the hilly Outaouais region with shallow soil near the bedrock [15]. The third terrain contains a drainage basin from the Abitibi region, a region with a relatively flat terrain and a high proportion of clay [4].

In order to validate the networks computed with this method, a comparison was done between the ESN and the traditional D8 flow accumulation method [27]. The D8 method was also chosen because the method was used to produce the networks that are the new reference in the hydrographic dataset published by the Ministère des Forêts, de la Faune et des Parcs du Québec, also available online. As mentionned in [2], single flow direction methods are preferred for high-resolution DTM. Hence, other approaches like D∞ [35] were not considered. For the ESN computation, the DTM was triangulated as in [17] to reduce the number of spurious pits.

Results for the D8 were produced with two different drainage enforcement methods. One result was obtained after filling the DTM with the Fill sinks XXL method [36] available in SAGA GIS, which completely fills all the depressions. The other result was obtained after breaching the DTM with the BreachDepressions tool of WhiteToolBox [21]. Breaching is done by tracing back a flow path from each pit and lowering the pixels along the flow path. These two networks are referred as the fill+D8 and the breach+D8 respectively.

In all cases, streams are initiated when the accumulation threshold is above 1.1 ha. This threshold was taken as the median drainage area from streams mapped in the field [20].

4.3 Results

4.3.1 Comparison of drainage networks

Computation of the drainage network from the surface network was done by selecting all thalwegs whose accumulation is above the threshold. The three drainage networks obtained from the ESN are presented in Figure 8.

As mentioned in section 3.3, puddles are mainly found in flat areas. Hence, in such places, the direction of the flow depends highly on the detection of puddles. Indeed, Table 1 shows the density of puddles in each terrain. The Kinonge terrain shows larger variations of elevations between 180 m and 354 m and contains far less puddles than the Abitibi terrain whose elevations are between 309 m and 324 m. The Berev terrain, which contains both hilly and flat regions, exhibits 52 puddles per hectare.

A consequence is that the complexity of the algorithm depends on the type of terrain and the number of pits. In flat areas, puddle computation requires a large number of

[1] https://www.foretouverte.gouv.qc.ca

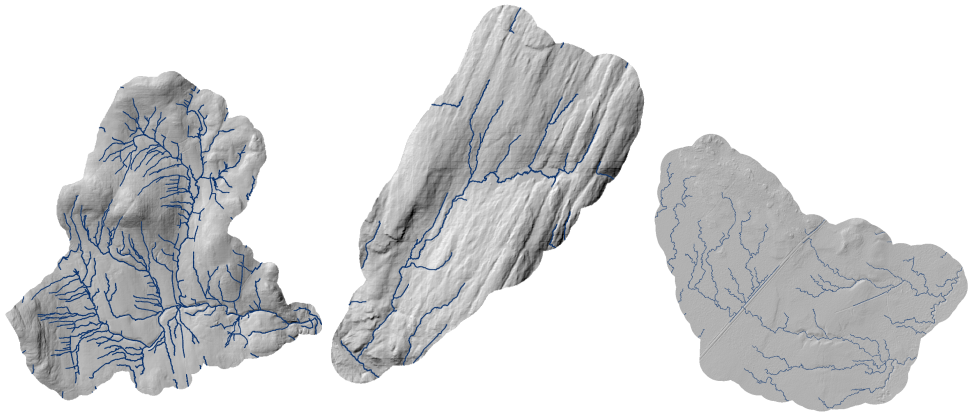

Figure 8: Drainage networks of the Berev, Kinonge and Abitibi terrains.

Table 1: Number of puddles per hectare in each DTM

Terrain	Puddles	Area (ha)	Puddles/ha
Berev	55627	1070	52
Kinonge	2698	109	25
Abitibi	28902	197	147

merges between the puddles. As seen in Figure 7, most puddles are formed of two to five close nodes and correspond to spurious pits seen as noise. However, puddles can also correspond to large depressions in the terrain found along the streams. Detecting such puddles demands more iterations and is heavier because building the puddle requires to go through all the nodes of the depression at each iteration. Examples of such puddles are presented in Figure 9. On the left, the puddle is formed along an embankment near a road. The culvert that passes under the road was not detected. The outlet of the puddle is located accross the road. On the right, the stream goes through a natural depression forming a wetland. In both cases, the puddle is about 1.5 m deep.

While flat areas, as in Figure 7 extracted from the Berev terrain, exhibit many thalwegs, the flow direction through the puddles was properly estimated and the result is close to the D8 network as shown in Figure 10.

In all cases, networks remain similar. The same streams were detected and the differences are only positional. Therefore, a measure of the error was performed with the Single Buffer Overlay Method [1]. The measure was done once with the filled network and once with the breached network. Since the D8 network is the reference network in each case, a buffer of one metre, corresponding to the raster resolution, was built around it. The accuracy is defined as the portion of the thalwegs that are inside the buffer and is given in Table 2.

Overall, the results in Table 2 show that the thalwegs coincide with the streams and that the accumulation computed in the ESN is correct. Only in the Abitibi DTM, a significant difference was observed between the ESN and fill+D8. This is mainly due to the filling method applied before the D8 computation. In a filled depression, streams tend to go in

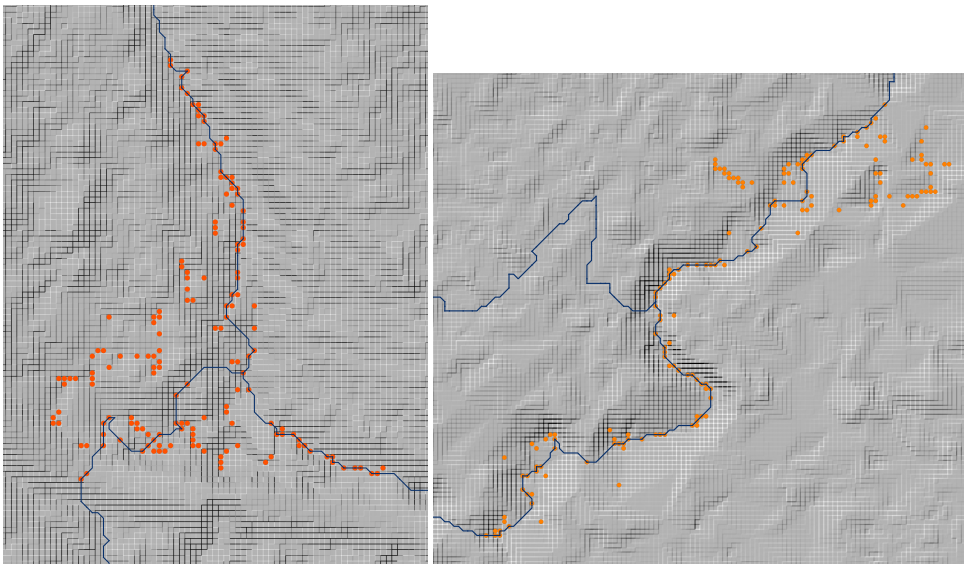

Figure 9: Large puddles found near an embankment and in a wetland along a stream.

Table 2: Positional accuracy of the thalwegs with reference to the fill+D8 and the breach+D8 networks.

Terrain	Fill+D8	Breach+D8
Berev	92.2%	93.6%
Kinonge	94.2%	96.6%
Abitibi	79%	94.7%

a straight line while breaching looks for a flow path out of the depression. This leads to a path that normally goes through the outlet of the depression and thus to a path following the natural slope, similar to the path computed by the thalweg (Figure 11).

In the Kinonge, errors are observed in a wetland. The surface is not completely flat with variations below the precision of the measurement, leading to a noisy surface that was filled in the fill+D8 approach. The other source of inaccuracy was located in hillslopes: streams were initiated earlier by the thalwegs than by the D8. Differences were also observed in the Berev where culverts are located. Culverts are not visible and the DTM was burnt to create a flow path. In places at the exit of the culverts, streams diverged leading to significant differences (Figure 12).

4.3.2 Strahler order and drainage basins

The Strahler order and drainage basins were also computed in the three case studies. Basins can be computed for any thalweg but are usually more relevant when computed at confluences of the drainage network. Figure 13 shows an example of basins computed for the Kinonge river. The Strahler network was first computed and then, the basin of each stream at different Strahler order was computed. The highest thalweg was chosen at the mouth

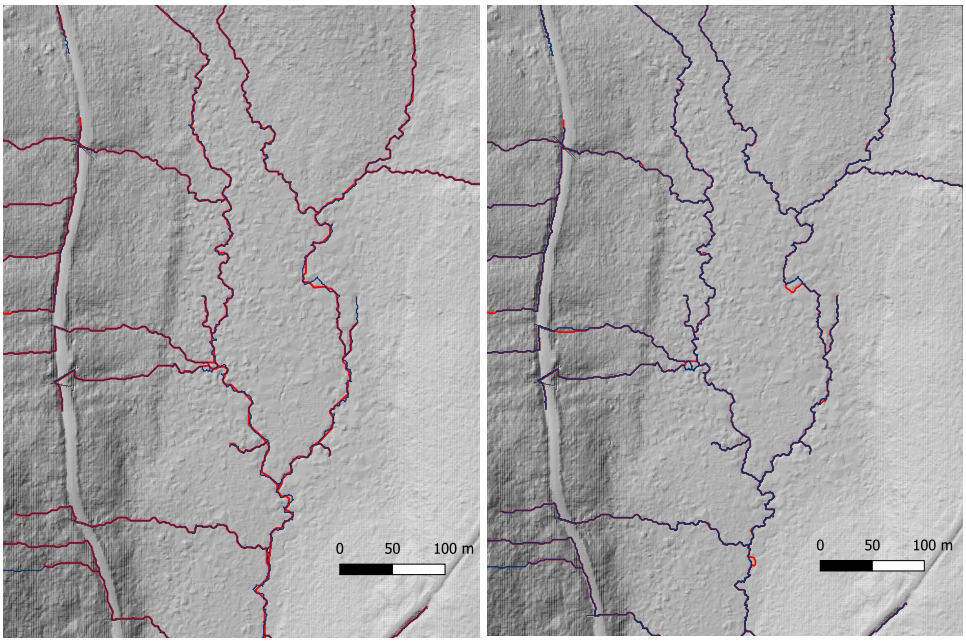

Figure 10: Streams obtained from thalwegs (blue) and fill+D8 (left) and breach+D8 (right).

of the river and its basin is the basin of the Kinonge river. Other basins are all subbasins within the first one.

4.4 Discussion

Results obtained in the case studies showed that the ESN can be used to extract streams from the DTM. The drainage network remains close to what is obtained with the D8 method. Even in flat areas, puddles permitted the computation of a flow that is consistent with D8. Differences of two sorts were observed. First, streams can vary because of the kind of drainage enforcement that was applied. Where filling was performed, streams tend to run in straight line across flat, filled depressions while breaching and thalwegs follow a flow path in the reverse way. Second, D8 and the ESN can compute different flow directions. These issues are observed at the exit of some culverts. Culverts are handled by burning the DTM, meaning that all pixels along the culvert are lowered at the same elevation. In our implementation, pixels at the same elevation are handled as in [34] by ordering the points according to their coordinates. The D8 relies on a different heuristic. Both decisions remain arbitrary and it is not possible to decide whether one is better than the other. It must be noted that areas where differences are observed often correspond to wetlands or even ponds or lakes. The position of the stream is strongly dependent on small variations in the surface and a lot of uncertainty remains in its accuracy [18]. Nonetheless, the ESN was still able to provide a valid solution and identified correctly the spring and the outlet of these surfaces.

The initiation of a stream depends on the accumulation threshold. Differences are also observed at channel heads because the threshold is not reached at the same place. When

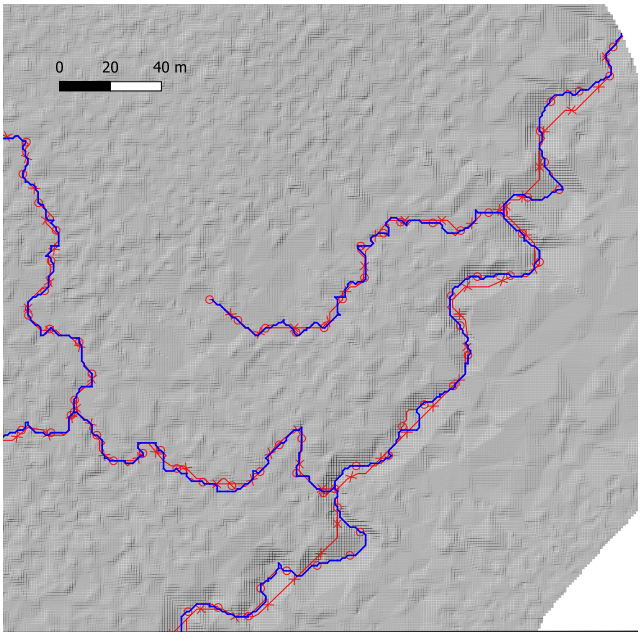

Figure 11: Streams defined by thalwegs (blue) and D8 in the Abitibi terrain (crosses: fill+D8, circles: breach+D8).

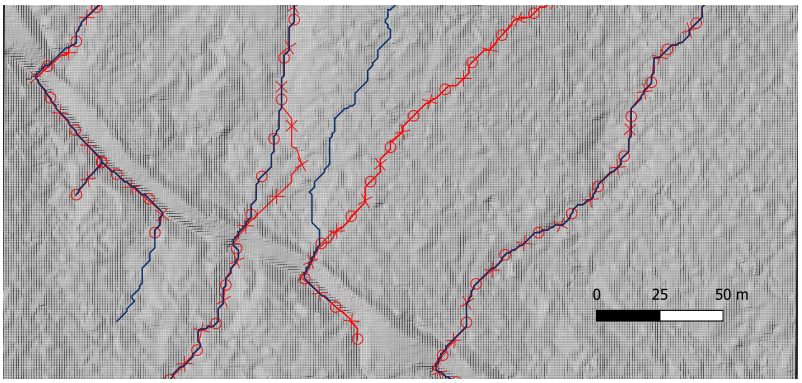

Figure 12: Streams exiting a culvert. Blue: thalwegs, red: D8 (crosses: fil+D8, circles: breach+D8).

these channel heads are located in slopes, these places correspond to head water streams and the streambed is not carved enough in the terrain, bringing again some uncertainty in its position and in the location of the spring [18].

The ESN can also compute other features such as drainage basins and the Strahler order. These features are not recorded in the ESN. While drainage basins can be computed for any thalweg, they are usually relevant only at confluences or at some points of interest for the user and can be easily extracted at any time from the ESN. Recording basins and dales

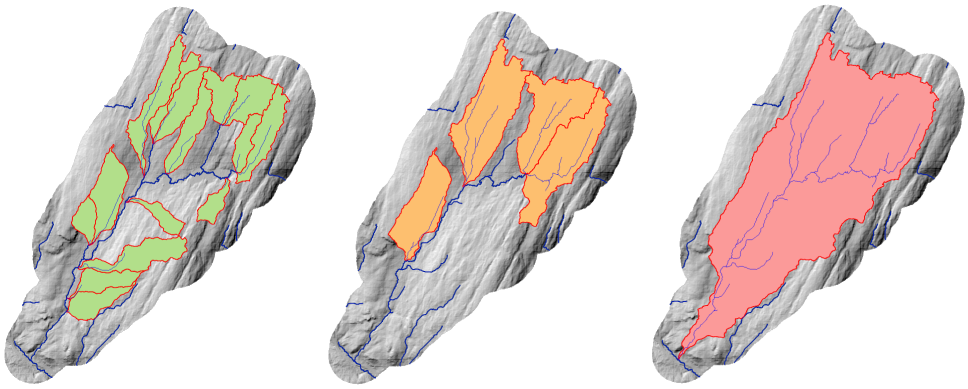

Figure 13: Basins of streams of Strahler order 1, 2 and 3.

would be redundant and basins being nested in each other, they do not define a simplicial complex as dales do. The Strahler order depends on the accumulation threshold. It would be possible to compute a Strahler order for all the thalwegs however, because there are many thalwegs in flat areas, this would lead to an artificially high order.

Indeed, handling flat areas is a weak point of the ESN as it is for other drainage computation methods. The ESN identifies many ridges and thalwegs because of the noise in the surface. This brings uncertainty in the position of the lines, which can greatly vary depending of the noise and shows a limitation in considering that topographic or hydrological features are represented by points and lines. Such areas may rather be identified as surfacic elements corresponding to transition areas or hydrological surfaces.

5 Conclusion

This paper introduced a new data structure that extends the surface network to embed both the surface network defined as a MSC and the drainage network. The ESN is still a simplicial complex that can be decomposed into a hill complex containing the thalweg network, and a dale complex containing the ridges. The thalweg network is defined as a weighted directed graph to define the flow direction and the flow accumulation. We showed that the drainage network extracted from the ESN is similar to the one extracted by the D8 approach. The ESN also allows the computation of other hydrographical features such as drainage basins. Furthermore, the ESN can be easily computed from either a raster or a TIN: the method presented here is applied on a triangulated grid and thus can also be applied to any triangulated network.

As such, the ESN answers the limitations mentioned in the introduction that were presented in [30]. A first limitation was the difficulty to build a topologically correct network. The ESN ensures a proper partition of the terrain in cells delineated by terrain features by imposing topological constraints on thalwegs and ridges. The second limitation was the fact that the MSC cannot be used to extract the drainage network that is commonly used in terrain analysis. The ESN provides a solution to this issue and thus allows the user to per-

form terrain analysis not only by relying on image-based approaches but also to develop graph-based approaches for landform detection. Such approaches would have the benefit of providing explicit relationships between terrain features and facilitate the identification of saliences characterizing the landforms.

In relation to the limitations mentioned in the previous section, a direction for future work is to integrate flat and slightly convex areas explicitly in the ESN [14]. This would allow for the integration of hydrological surfaces in the drainage network directly and a better understanding of where diffluences are possible. However, this would rely on a proper delineation of these surfaces. Another issue to improve the definition of the drainage is the integration of culverts. Instead of burning the terrain where culverts are, they could be directly integrated in the surface network to impose a flow in the right direction at these places.

A second direction concerns terrain analysis. The ESN provides a segmentation of the terrain into dales and hills that can be seen as landform elements and are all connected in a graph. Thalwegs and ridges can also be seen as saliences of the terrain. Hence, new terrain analysis techniques relying on graph analysis will be explored, specifically to study landforms created by fluvial erosion.

Acknowledgments

The research presented here is supported by grant 2021-PR-282427 from the FRQNT (Fonds de Recherche Nature et Technologies Québec). The first author also acknowledges support from the NSERC (Natural Sciences and Engineering Research Council) Discovery grant 2016-05129.

References

[1] ARIZA-LÓPEZ, F., AND MOZAS-CALVACHE, A. Comparison of four line-based positional assessment methods by means of synthetic data. *Geoinformatica 16* (2012), 221–243. doi:10.1007/s10707-011-0130-y.

[2] ARIZA-VILLAVERDE, A. B., JIMÉNEZ-HORNERO, F. J., AND GUTIÉRREZ DE RAVÉ, E. Influence of DEM resolution on drainage network extraction: A multifractal analysis. *Geomorphology 241* (2015), 243–254. doi:10.1016/j.geomorph.2015.03.040.

[3] BARBER, C. P., AND SHORTRIDGE, A. Lidar elevation data for surface hydrologic modeling: Resolution and representation issues. *Cartography and Geographic Information Science 32*, 4 (2005), 401–410. doi:10.1559/152304005775194692.

[4] BLOUIN, J., AND BERGER, J.-P. *Guide de reconnaissance des types écologiques des régions écologiques 5a - Plaine de l'Abitibi*. Ministère des ressources naturelles du Québec, Québec, 2004.

[5] BLOUIN, J., AND BERGER, J.-P. *Guide de reconnaissance des types écologiques des régions écologiques 5e - Massif du lac Jacques-Cartier et 5f - Massif du mont Valin*. Ministère des ressources naturelles du Québec, Québec, 2004.

[6] BRÄNDLI, M. Hierarchical models for the definition and extraction of terrain features. In *Geographic Objects With Indeterminate Boundaries* (London, 1996), Taylor & Francis, pp. 257–270.

[7] BREMER, P.-T., EDELSBRUNNER, H., HAMANN, B., AND PASCUCCI, V. A topological hierarchy for functions on triangulated surfaces. *IEEE Transactions on Visualization and Computer Graphics 10*, 4 (2004), 385–396. doi:10.1109/TVCG.2004.3.

[8] CAYLEY, A. On contour and slope lines. *The London, Edinburgh, and Dublin Philosophical Magazine and Journal of Science 18* (1859), 264–268. doi:10.1080/14786445908642760.

[9] CLARKE, K. C., AND ROMERO, B. E. On the topology of topography: a review. *Cartography and Geographic Information Science 44*, 3 (2017), 271–282. doi:10.1080/15230406.2016.1164625.

[10] ČOMIĆ, L., DE FLORIANI, L., MAGILLO, P., AND IURICICH, F. *Morphological Modeling of Terrains and Volume Data*. SpringerBriefs in Computer Science. Springer, New York, 2014. doi:10.1007/978-1-4939-2149-2.

[11] CORTÉS MURCIA, A. C., GUILBERT, E., AND MOSTAFAVI, M. A. An object based approach for submarine canyon identification from surface networks. In *Short paper proceedings of the Ninth international conference on GIScience* (Berkeley, 2016), eScholarship, University of California, pp. 60–63. doi:10.21433/B31105h6f9b1.

[12] DANOVARO, E., DE FLORIANI, L., MAGILLO, P., MESMOUDI, M. M., AND PUPPO, E. Morphology-driven simplification and multiresolution modeling of terrains. In *The 11th International Symposium on Advances in Geographic Information Systems* (2003), E. Hoel and P. Rigaux, Eds., ACM press, pp. 63–70. doi:1-58113-730-3/03/0011.

[13] FAIRFIELD, J., AND LEYMARIE, P. Drainage networks from digital elevation models. *Water resources research 27*, 5 (1991), 709–717. doi:10.1029/90WR02658.

[14] GONZALEZ-DIAZ, R., BATAVIA, D., CASABLANCA, R. M., AND KROPATSCH, W. G. Characterizing slope regions. *Journal of Combinatorial Optimization* (2021). doi:10.1007/s10878-021-00783-5.

[15] GOSSELIN, J. *Guide de reconnaissance des types écologiques des régions écologiques 4b - Coteaux du réservoir Cabonga et 4c - Collines du Moyen-Saint-Maurice*. Ministère des ressources naturelles du Québec, Québec, 2002.

[16] GUILBERT, E. Surface network extraction from high resolution digital terrain models. *Journal of spatial information science 22* (2021), 33–59. doi:10.5311/JOSIS.2021.22.681.

[17] GUILBERT, E., JUTRAS, S., AND BADARD, T. Thalweg detection for river network cartography in forest from high-resolution lidar data. In *ISPRS - International Archives of the Photogrammetry, Remote Sensing and Spatial Information Sciences* (Germany, 2018), vol. XLII-4, Copernicus Publications, pp. 241–247. doi:10.5194/isprs-archives-XLII-4-241-2018.

[18] HENGL, T., HEUVELINK, G. B. M., AND VAN LOON, E. E. On the uncertainty of stream networks derived from elevation data: The error propagation approach. *Hydrology and Earth System Sciences 14*, 7 (2010), 1153–1165. doi:10.5194/hess-14-1153-2010.

[19] HUTCHINSON, M. A new method for gridding elevation and stream line data with automatic removal of spurious pits. *Journal of Hydrology 106*, 3–4 (1989), 211–232. doi:10.1016/0022-1694(89)90073-5.

[20] LESSARD, F. Optimisation cartographique de l'hydrographie linéaire fine. Master's thesis, Université Laval, 2020.

[21] LINDSAY, J. B. Efficient hybrid breaching-filling sink removal methods for flow path enforcement in digital elevation models. *Hydrological Processes 30*, 6 (2016), 846–857. doi:10.1002/hyp.10648.

[22] LINDSAY, J. B., FRANCIONI, A., AND COCKBURN, J. M. H. Lidar DEM smoothing and the preservation of drainage features. *Remote Sensing 11*, 1926 (2019). doi:10.3390/rs11161926.

[23] LYU, F., XU, Z., MA, X., WANG, S., LI, Z., AND WANG, S. A vector-based method for drainage network analysis based on lidar data. *Computers and geosciences 156* (2021), 10 pages. doi:10.1016/j.cageo.2021.104892.

[24] MAXWELL, J. C. On hills and dales. *The London, Edinburgh, and Dublin Philosophical Magazine and Journal of Science 40* (1870), 421–427. doi:10.1080/14786447008640422.

[25] MORSE, M. Relations between the critical points of a real function on n independent variables. *Transactions of the American Mathematical Society 27* (1925), 345–396. doi:10.2307/1989110.

[26] NORGARD, G., AND BREMER, P.-T. Robust computation of Morse-Smale complexes of bilinear functions. *Computer Aided Geometric Design 30* (2013), 577–587. doi:10.1016/j.cagd.2012.03.017.

[27] O'CALLAGHAN, J. F., AND MARK, D. M. The extraction of drainage networks from digital elevation data. *Computer vision, graphics and image processing 28* (1984), 323–344. doi:10.1016/S0734-189X(84)80011-0.

[28] PFALTZ, J. Surface networks. *Geographical Analysis 8* (1976), 77–93. doi:10.1111/j.1538-4632.1976.tb00530.x.

[29] QUINN, P., BEVEN, K., CHEVALLIER, P., AND PLANCHON, O. The prediction of hillslope flow paths for distributed hydrological modelling using digital terrain models. *Hydrological Processes 5* (1991), 59–79. doi:10.1002/hyp.3360050106.

[30] RANA, S. Issues and future directions. In *Topological data structures for surfaces. An introduction to geographical information science* (Chichester, 2004), S. Rana, Ed., Wiley, pp. 179–183.

[31] SCHNEIDER, B. Surface networks: extension of the topology and extraction from bilinear surface patches. In *Proceedings of the 7th international conference on GeoComputation* (2003). doi:10.1.1.89.9824.

[32] SINHA, G., AND MARK, D. M. Cognition-based extraction and modelling of topographic eminences. *Cartographica 45*, 2 (2010), 105–112. doi:10.3138/carto.45.2.105.

[33] STRAHLER, A. N. Quantitative analysis of watershed geomorphology. *Transactions of the American Geophysical Union 8*, 6 (1957), 913–920. doi:10.1029/TR038i006p00913.

[34] TAKAHASHI, S., IKEDA, T., SHINAGAWA, Y., KUNII, T. L., AND UEDA, M. Algorithms for extracting correct critical points and constructing topological graphs from discrete geographical elevation data. *Computer Graphics Forum 14* (1995), 181–192. doi:10.1111/j.1467-8659.1995.cgf143_0181.x.

[35] TARBOTON, D. G. A new method for determination of flow directions and upslope in grid elevation models. *Water Resources Research 33*, 2 (1997), 309–319. doi:10.1029/96WR03137.

[36] WANG, L., AND LIU, H. An efficient method for identifying and filling surface depressions in digital elevation models for hydrologic analysis and modelling. *International Journal of Geographical Information Science 20*, 2 (2006), 193–213. doi:10.1080/13658810500433453.